A SELF-REFERENCING LEVEL-SET METHOD FOR IMAGE RECONSTRUCTION FROM SPARSE FOURIER SAMPLES [1]

Jong Chul Ye, Yoram Bresler and Pierre Moulin

Coordinated Science Laboratory, University of Illinois at Urbana-Champaign, IL 61801
Email: {jong,yoram,moulin}@ifp.uiuc.edu

ABSTRACT

We address image estimation from sparse Fourier samples. The problem is formulated as joint estimation of the supports of unknown sparse objects in the image, and pixel values on these supports. The domain and the pixel values are alternately estimated using the level-set method and the conjugate gradient method, respectively. Our level-set evolution shows a unique switching behavior, which stabilizes the level-set evolution and removes the re-initialization steps in conventional level set approaches.

1. INTRODUCTION

In Fourier imaging problems, the goal is to reconstruct an image from samples of its Fourier transform. Examples include synthetic aperture radar (SAR), radio astronomy, and magnetic resonance imaging (MRI). If a sufficient number of Fourier samples are available, the reconstruction can be easily obtained using the inverse Fourier transform. However, in many practical situations, owing to physical or economic limitations, only a small number of Fourier samples is available.

With sparse Fourier data, the reconstruction problem becomes ill-posed, because it does not admit a unique solution. However, if the image can be assumed to consist of objects supported on a small unknown set D on a known background, a unique solution exists, provided the sampling pattern satisfies appropriate so-called universality conditions [1]. These conditions are typically satisfied by random sampling patterns. The computation of the reconstruction requires, however, the solution of a difficult nonlinear problem.

An alternative approach to such problems developed over the past decade is based on edge preserving regularization (EPR) [2]. However, EPR does not make explicit use of the prior knowledge of sparse objects on a homogeneous background, and therefore may not offer optimum performance with sparse data. Instead, in this paper we explicitly use this prior knowledge, and formulate the problem as the estimation of the support D as well as the pixel values in it. To solve the associated nonlinear problem, we derive a gradient-based nonlinear optimization technique, where we alternately estimate the domain D and the pixel values using a level-set evolution method and the conjugate gradient (CG) technique, respectively.

Related work on domain estimation algorithm using level-set approaches has appeared in [3], which considers a binary image. Our approach addresses a more general problem, where both support domain and pixel values are unknown, and are estimated jointly. In addition to reconstructing non-constant objects, our approach allows to reconstruct objects on a known non-homogeneous background, neither of which is possible using the approach in [3]. The latter feature is important in tasks of "change detection" in a reference image acquired at an earlier time. Furthermore, in our level-set approach the embedding level function is initialized using the direct Fourier inversion estimate of pixel value, rather than the conventional signed distance function. This formulation has several unique advantages. First, the initialization of the level-set and the necessary extension of the evolution velocity are simplified. Second, the resultant level-set evolution shows a switching behavior with significant stabilizing effects, hence the level function is never re-initialized. Finally, by combining with CG steps of pixel value update, the stability and the speed of the level-set evolution can be easily controlled by the number of the CG steps. For more details about this work, please refer to [4].

2. PROBLEM FORMULATION

Let $\Omega \subset \mathbb{R}^2$ denote the image domain and the open set D a subset (which may be disconnected) of Ω. Suppose the unknown image $v(\mathbf{x})$ ($\mathbf{x} \in \Omega$) has the following form:

$$u(\mathbf{x}) = \begin{cases} v(\mathbf{x}), & \mathbf{x} \in D \\ 0 & \mathbf{x} \in \Omega \backslash D \end{cases} \tag{1}$$

where $v(\mathbf{x})$ is an unknown pixel value at $\mathbf{x} \in D$. Thus, the objects may have arbitrary values over their support. The model (1) includes more general cases of known background since in those cases the unknown image $u(\mathbf{x})$ of (1) can be regarded as the unknown difference image. The noiseless measurement in the Fourier imaging problem is given by:

$$F^D v(\mathbf{f}) = \int_D \exp\left(-j\mathbf{f}\cdot\mathbf{x}'\right) v(\mathbf{x}')d\mathbf{x}' \quad , \quad \mathbf{f} \in \Phi \subset \mathbb{R}^2 \tag{2}$$

where $\mathbf{f} \in \mathbb{R}^2$ is the frequency, Φ denotes the set of 2-D frequency sample locations, and $d\mathbf{x}'$ denotes the differential surface element. Suppose we have noisy samples $y(\mathbf{f}), \mathbf{f} \in \Phi$. Our goal is to fit (2) to the noisy samples while penalizing the length of the boundary of the domain D. The resultant penalized least-squares estimator of D and v can be computed by

$$\min_{D,v} \left(\frac{1}{2} ||y - F^D v||_\Phi^2 + \alpha \int_\Gamma d\Gamma \right) \tag{3}$$

[1] This work was supported in part by a grant from DARPA under Contract F49620-98-1-0498, administered by AFOSR, and by a NSF Research Infrastructure Grant No. CDA 96-24396.

where $||z||_\Phi^2 = \int_\Phi |z(\mathbf{f})|^2 d\mathbf{f}$, the second integral is a line-integral along the boundary $\Gamma = \partial D$ (hence the length of the domain boundary), and α is a regularization constant. This form of penalized likelihood can be motivated in various ways, including one based on Risannen's minimum description length (MDL) [5].

3. ALTERNATING MINIMIZATION

To solve the optimization problem (3), we use an alternating minimization of the cost function with respect to the pixel value v and the domain D. For fixed D, the optimization problem is simple, admitting the linear least-squares solution

$$\hat{v} = \left(F^D\right)^\dagger y \tag{4}$$

where $A^\dagger$ denotes the pseudo inverse of A and $\hat{v}$ is defined only on D. Because of the large dimensions of the matrix involved in the discrete form of (4), the estimator $\hat{v}$ of (4) is preferably obtained using the conjugate gradient algorithm, without ever having to form the matrix itself.

4. SHAPE DERIVATIVES

4.1. Shape Deformation

A shape deformation is described by constructing a family of shapes $D_t, D_0 = D$ that are perturbations of D for $0 \leq t < \epsilon$, t being a fictitious time parameter. More specifically, we have $D_t = \{\mathbf{x}(t)\}$ where $\mathbf{x}(t)$ denotes the solution to the system of ordinary differential equations

$$\frac{d\mathbf{x}(t)}{dt} = V(t, \mathbf{x}(t)), \quad \mathbf{x}(0) \in D \ . \tag{5}$$

Then, the following result from shape analysis allows us to use a gradient-based approach for the domain update:

Proposition 1 (Sokolowski and Zolesio [6]) *Let the domain functions $Q(D)$ and $L(D)$ be given by*

$$Q(D) = \int_D Y d\mathbf{x} \quad , \quad L(D) = \int_\Gamma Y d\Gamma \ , \tag{6}$$

where Γ is of class C^1. Suppose D_t is deformed by (5). Then, the domain functions $Q(D)$ and $L(D)$ are shape differentiable,

$$Q'(D,V) = \left(\frac{\partial}{\partial t}\int_{D_t} Y d\mathbf{x}\right)_{t=0} = \int_\Gamma Y \boldsymbol{F}\, d\Gamma \tag{7}$$

$$L'(D,V) = \int_\Gamma \kappa Y \boldsymbol{F}\, d\Gamma, \tag{8}$$

where $\boldsymbol{F} =< V(0), n >$ denotes the component of the velocity normal to the boundary Γ at $t = 0$, n denotes outer normal vector on Γ, and κ denotes the curvature of Γ.

4.2. Shape Derivatives of the Cost Functional

We wish to obtain a closed form for the derivatives of the cost functional (3) with respect to a perturbation of the geometry. Using Proposition 1, the steepest descent direction of the domain update for the minimization problem (3) is given by a normal boundary speed function $\boldsymbol{F}(x)$ (boundary flow) of the form

$$\boldsymbol{F} = -(E + \alpha\kappa)\,\chi_\Gamma \tag{9}$$

$$E = Re\left[v^*\left(F^D\right)^*\left(F^D v - y\right)\right] \tag{10}$$

where χ_Γ denotes the indicator function of the boundary Γ.

5. SELF-REFERENCING LEVEL-SET METHOD

5.1. Shape Evolution by Level-Sets

Rather than evolve the boundary directly, we adopt the powerful level-set approach pioneered by Sethian and Osher [7], where for a given boundary flow $\boldsymbol{F}$, the evolution of the domain is then given by

$$\frac{\partial \phi}{\partial t} = -\boldsymbol{F}\,|\nabla\phi| \ . \tag{11}$$

In (11) the zero level set $\left\{\mathbf{x} \in \mathbb{R}^2 | \phi(t,\mathbf{x}) = 0\right\}$ corresponds to the boundary Γ_t. Using (11), topological changes of the domain evolution can be handled easily. Furthermore, the level-set algorithm can be implemented in a fixed Cartesian grid throughout the iterative process. For our problem, $\boldsymbol{F}$ is given by (9).

5.2. The Velocity Extension Problem

In a level set formulation, not only is the interface embedded in a higher dimensional function, but the normal speed of the interface is itself embedded in a higher dimensional function. Sethian [7] proposed a fast extension method of the velocity which preserves the signed distance in narrow band around the zero level curve (In this approach, the initialization of the level set is given by a signed distance function).

However, neither the signed distance, nor this choice of velocity extension are effective for our problem, because the level function must be re-initialized after several iterations to preserve the signed distance. The advantage of our approach over such re-initialization is the "switching" behavior of our level-set evolution, which keeps the level function stable avoiding the problematic re-initialization step.

5.3. Velocity Extension

Recall the normal velocity field (9). One may think that a simple extension of (10) to the whole domain Ω is obtained by removing the indicator function:

$$-\left(Re\left[v^*\left(F^D\right)^*\left(F^D v - y\right)\right] + \alpha\kappa\right) \ . \tag{12}$$

However, since the image estimate v is restricted to D, the first term in (12) is only defined on D.

A straightforward velocity extension method using (12) is given by $\boldsymbol{F}_e = -(E_e + \alpha\kappa)$ where E_e is computed as

$$Re\left[v^*\left(F^D\right)^*\left(F^D v - y\right)\right] + Re\left[w^*\left(F^{\Omega\setminus D}\right)^*\left(F^D v - y\right)\right] \ , \tag{13}$$

for some nonzero complex-valued function w defined on $\Omega \setminus D$, and $\left(F^\Omega\right)^* = \left(F^D\right)^* + \left(F^{\Omega\setminus D}\right)^*$. Using (13), the level set evolution is now given by

$$\frac{\partial \phi}{\partial t} = E_e|\nabla\phi| + \alpha\kappa|\nabla\phi| \ . \tag{14}$$

In order to avoid technical difficulties such as scaling and phase mismatch, a good candidate for w is an estimate of v defined on $\Omega \setminus D$ or Ω.

5.4. A Self-Referencing Level-Set Method

In many Fourier imaging problem, the inverse Fourier transform image

$$\hat{u}_0 = (F^{\Omega})^{-1} y = (F^{\Omega})^* y \ , \tag{15}$$

is used as a reconstructed image. Therefore, one idea is to use (15) to initialize the level function. Indeed such a formulation of the level function has several advantages over the signed distance function because the new level function has approximate information about the image intensity.

Based on this observation, we define an image magnitude function $m(t, \mathbf{x})$, and initialize it to the magnitude of the inverse Fourier reconstruction of (15), $m(0, \mathbf{x}) = |\hat{u}_0(\mathbf{x})|$. We then pick the level-set function to be

$$\phi(t, x) = g[m(t, \mathbf{x})] \quad \forall t \geq 0 \tag{16}$$

where $g : \mathbb{R}^+ \to \mathbb{R}$ is a decreasing invertible continuous differentiable function. For example, an adequate choice might be $g(z) = T_H - z$, where T_H is an appropriate threshold value, which is less than the maximum value of $m(0, \mathbf{x}) = |w(0, \mathbf{x})|$. This choice then initializes the level set to

$$\phi(0, \mathbf{x}) = g[m(0, \mathbf{x})] \quad , \quad m(0, \mathbf{x}) = |\hat{u}_0(\mathbf{x})| \ . \tag{17}$$

Then, we can show that the magnitude function $m = g^{-1}(\phi)$ is a solution to the following evolution equation:

$$\frac{\partial m}{\partial t} = -E_e |\nabla m| + \alpha \kappa_m |\nabla m|, \tag{18}$$

$$m(0, \mathbf{x}) = |\hat{u}_0(x)| \tag{19}$$

where κ_m denotes the curvature of $m(t, \mathbf{x})$.

Note that the flow (18) and (19) is an anisotropic diffusion of the magnitude image $|\hat{u}_0(\mathbf{x})|$ produced by direct Fourier inversion. Based on this observation, we propose to use $m(t, \mathbf{x})$ as an estimate of the image magnitude $|w(t, \mathbf{x})|$ on $\Omega \setminus D$. Now, by assuming that the phase of the image on $\Omega \setminus D$ does not change significantly during the evolution, we obtain the following evolution for $w(t, \mathbf{x})$:

$$w(t, \mathbf{x}) = m(t; \mathbf{x}) e^{\jmath \angle \hat{u}_0(\mathbf{x})} \ , \tag{20}$$

where $\angle$ denotes the argument of a complex quantity.

Because the level function is initialized as a function of the image estimate (rather than e.g., a signed distance function), we will call this level-set formulation a *self-referencing level set* method.

5.5. Stability of Level Function

Recall that for the choice of the signed distance function as a level function, periodic re-initialization is performed to maintain the signed distance, and hence stabilize the evolution [7]. The main contribution of our algorithm is that such re-initialization steps are not necessary. Note that by substituting (4) into (13), we can show that our level-set evolution is given by

$$\frac{\partial \phi}{\partial t}(t, \mathbf{x}) = \begin{cases} \alpha \kappa |\nabla \phi(t, \mathbf{x})|, & \mathbf{x} \in D \\ (E_e + \alpha \kappa) |\nabla \phi(t, \mathbf{x})|, & \mathbf{x} \notin D \end{cases} \ , \tag{21}$$

since $\left(F^D\right)^* P_D^{\perp} = 0$. Eq. (21) tells us that if $\mathbf{x} \notin D$ the level-set evolution is driven by the data-driven force E_e and the roughness of the level-set $|\nabla \phi|$. If the estimate of D is incorrect, there will be data mismatch (i.e., $P_D^{\perp} y \neq 0$) resulting in a nonzero data-driven force E_e and allowing the level-set to keep evolving. However, for $\mathbf{x} \in D$ the curvature flow will stabilize the level-set evolution. This "switching" controls the minimum value of the level function. More specifically, consider the adequate choice $g(z) = T_H - z$ with T_H constant throughout the evolution iteration. Then, we can show that asymptotically the minimum vale of the level function is zero, hence $\max_{\mathbf{x} \in \Omega} \lim_{t \to \infty} |w(t, \mathbf{x})| = T_H$.

Another advantage of our algorithm is that the "switching" effect can be easily controlled by the number of CG steps. For examples, if a small number of CG steps are used, $\hat{v} \neq (F^D)^{\dagger} y$ and the contribution of F on D may be significant. This tends to allow rapid evolution of the level function. On the contrary, for large number of CG steps, the contribution of F becomes negligible, hence the level function is stabilized.

6. NUMERICAL RESULTS

Once the velocity is chosen, all coefficients that are involved in (14) are defined. Then, (14) is discretized with "upwinding" finite difference [7]. We use the function $g(z) = T_H - z$ for all our simulation where T_H is a threshold value, which is set depending on each problem. The regularization parameter α in (14) is hand-picked for best performance. To describe the experiments, we introduce the following definitions. For $N \times N$-pixel image we measure region sizes, $|D|$ $|\Phi|$ and $|\Omega| = N^2$ by the number of pixels they contain. The fraction $\eta = |D|/N^2$ of the image occupied by the supports of the objects is called the *occupancy rate*. Likewise, because the total number of Fourier samples is $|\Phi|$, we call $\rho = |\Phi|/N^2$ the *sampling rate*. Theoretical analysis indicates that reliable reconstruction requires $\rho > \eta$, often by some factor [8].

Example 1. The test image is generated by cutting the Lena image as shown in Fig. 1. The pixel values are normalized to have maximum value of 2. The domain D, occupancy, and the noise level are all the same as in Example 1. We reduce the sampling rate down to $\rho = 37.5\% = 1.5\eta$. Again, while the direct Fourier inversion (Fig. 1(b)) is blurry, the reconstruction by our algorithm after 200 iteration (Fig. 1(c)) is accurate. The domain estimate (Fig. 1(d)) are also quite accurate.

Example 2. This example is drawn from a SAR imaging problem. The pixel values are normalized to have the maximum magnitude of 2, and additive complex Gaussian noise is added to the samples at an rms level of 5%. The occupancy rate is now $\eta = 37\%$, but the sampling rate is only $\rho = 0.33\eta$. This is a severely undersampled case, which according to theory [8] does not suffice for reconstruction of even one third of the object support. A true VFY aircraft reflectance image and the direct Fourier inversion result are given in Figs. 2(a)(b). The reconstruction by our algorithm after 100 iterations (Fig. 2(c)) shows important parts of the structure of the VFY aircraft.

Example 3. This example is drawn from a magnetic resonance imaging problem. The goal is "change detection" in a complex background, which is however known, from previous reference scans. Consider the "Shepp-Logan" phantom given in Fig. 3(a) with three "tumors", which have *unknown* additional absorption values of 0.5, 0.6, and 1.0

and unknown supports. Assuming that we know the original healthy phantom without tumors, our goal is now to estimate the image in Fig. 3(a) from its noisy Fourier samples. Again, additive complex Gaussian noise is added to the samples at an rms level of 5%. The occupancy rate of the difference image - which corresponds to three tumors - is now $\eta = 2.3\%$, and the sampling rate is only $\rho = 2\eta = 4.6\%$. A Fourier reconstruction in Fig. 3(b) is very poor and we cannot locate any tumors, because of the poor point spread function of the system. However, the reconstruction after 100 iterations using the new method (Figs. 3(c)) is still good.

7. CONCLUSION

We introduced a new algorithm for image estimation from sparse Fourier samples. The problem was formulated as joint estimation of the supports of unknown sparse objects in the image, and pixel values on these support. The domain and the pixel values are alternately estimated using what we call the self-referencing level-set method and the conjugate gradient method, respectively. Our level function was initialized as a function of the magnitude of the direct Fourier inversion results. This choice totally removes the reinitialization step in conventional level set methods. Simulation results suggest that our algorithm provides accurate image and domain estimates from sparse Fourier samples (close to the theoretical minimum) and is quite robust to noise.

REFERENCES

[1] R. Venkataramani and Y. Bresler, "Further results on spectrum blind sampling of 2D signals," *Proc. IEEE Int. Conf. Image Proc., ICIP*, vol. 2, Oct. 1998, Chicago, pp. 752–756.

[2] A. H. Delaney and Y. Bresler, "Globally convergent edge-preserving regularized reconstruction: An application to limited-angle tomography," *IEEE Trans. on Image Processing*, no. 2, pp. 204–221, February 1998.

[3] F. Santosa, "A level-set approach for inverse problems involving obstacles," *ESAIM: Control, Optimisation and Calculus of Variations*, pp. 17–33, January 1996.

[4] J. Ye, Y. Bresler, and P. Moulin, "A self-refencing level-set method for image reconstruction from sparse Fourier samples," *to appear in Proc. IEEE Workshop in Variational and Level Set Methods in Computer Vision*, July 2001, Vancouver, Canada.

[5] Y. G. LecLerc, "Constructing simple stable descriptions for image partitioning," *International Journal of Computer Vision*, pp. 73–102, 1989.

[6] J. Sokolowski and J. Zolesio, *Introduction to Shape Optimization: Shape Sensitivity Analysis*. New York: Springer-Verlag, 1991.

[7] J. A. Sethian, *Level Set Methods and Fast Marching Methods*. United Kingdom: Cambridge University Press, 1996.

[8] M. Gastpar and Y. Bresler, "On the necessary density for spectrum-blind nonuniform sampling subject to quantization," *Proc. of IEEE Int'l Conf. on Acoust., Speech and Sig. Proc.*, June 2000, Istanbul.

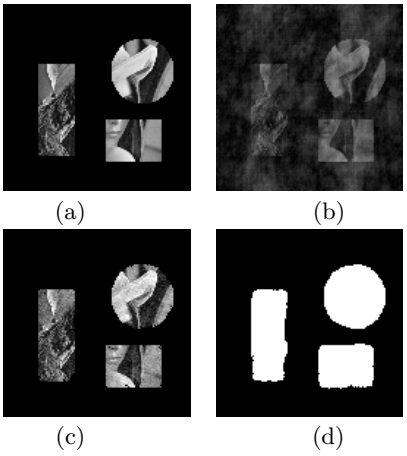

Figure 1: Example 1 (a) partial Lena image, (b) direct Fourier inversion, (c) reconstruction by our algorithm, and (d) the estimated domain.

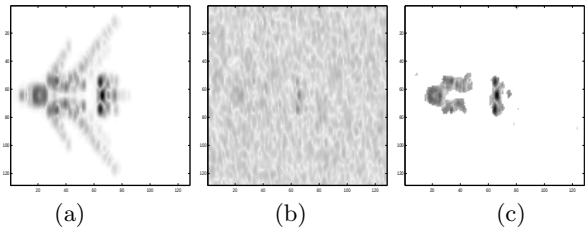

Figure 2: Example 2 (a) original VFY aircraft image, (b) direct Fourier reconstruction, and (c) reconstruction by our algorithm.

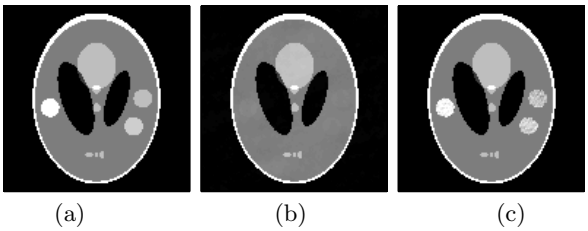

Figure 3: Example 3 (a) original phantom image with tumors, (b) direct Fourier reconstruction, and (c) reconstruction by our algorithm.